Title

Magnetic Resonance Imaging of Optic Nerve Traction During Adduction in Primary Open-Angle Glaucoma With Normal Intraocular Pressure

Journal

Investigative Ophthalmology & Visual Science, 58(10)

ISSN

0146-0404

Authors

Demer, Joseph L
Clark, Robert A
Suh, Soh Youn
et al.

Publication Date

2017-08-22

DOI

10.1167/iovs.17-22093

Peer reviewed

Magnetic Resonance Imaging of Optic Nerve Traction During Adduction in Primary Open-Angle Glaucoma With Normal Intraocular Pressure

Joseph L. Demer,[1–5] Robert A. Clark,[1,2] Soh Youn Suh,[1] JoAnn A. Giaconi,[1,2] Kouros Nouri-Mahdavi,[1,2] Simon K. Law,[1,2] Laura Bonelli,[1,2] Anne L. Coleman,[1,2] and Joseph Caprioli[1,2]

[1]Department of Ophthalmology, University of California, Los Angeles, California, United States
[2]Stein Eye Institute, University of California, Los Angeles, California, United States
[3]Biomedical Engineering Interdepartmental Program, University of California, Los Angeles, California, United States
[4]Neuroscience Interdepartmental Program, University of California, Los Angeles, California, United States
[5]Department of Neurology, University of California, Los Angeles, California, United States

Correspondence: Joseph L. Demer, Stein Eye Institute, 100 Stein Plaza, UCLA, Los Angeles, CA 90095, USA; jld@jsei.ucla.edu.

Submitted: April 21, 2017
Accepted: July 28, 2017

Citation: Demer JL, Clark RA, Suh SY, et al. Magnetic resonance imaging of optic nerve traction during adduction in primary open-angle glaucoma with normal intraocular pressure. *Invest Ophthalmol Vis Sci*. 2017;58:4114–4125. DOI:10.1167/iovs.17-22093

Purpose. We used magnetic resonance imaging (MRI) to ascertain effects of optic nerve (ON) traction in adduction, a phenomenon proposed as neuropathic in primary open-angle glaucoma (POAG).

Methods. Seventeen patients with POAG and maximal IOP $\leq$ 20 mm Hg, and 31 controls underwent MRI in central gaze and 20° to 30° abduction and adduction. Optic nerve and sheath area centroids permitted computation of midorbital lengths versus minimum paths.

Results. Average mean deviation (±SEM) was −8.2 ± 1.2 dB in the 15 patients with POAG having interpretable perimetry. In central gaze, ON path length in POAG was significantly more redundant (104.5 ± 0.4% of geometric minimum) than in controls (102.9 ± 0.4%, $P = 2.96 \times 10^{-4}$). In both groups the ON became significantly straighter in adduction (28.6 ± 0.8° in POAG, 26.8 ± 1.1° in controls) than central gaze and abduction. In adduction, the ON in POAG straightened to 102.0% ± 0.2% of minimum path length versus 104.5% ± 0.4% in central gaze ($P = 5.7 \times 10^{-7}$), compared with controls who straightened to 101.6% ± 0.1% from 102.9% ± 0.3% in central gaze ($P = 8.7 \times 10^{-6}$); and globes retracted 0.73 ± 0.09 mm in POAG, but only 0.07 ± 0.08 mm in controls ($P = 8.8 \times 10^{-7}$). Both effects were confirmed in age-matched controls, and remained significant after correction for significant effects of age and axial globe length ($P = 0.005$).

Conclusions. Although tethering and elongation of ON and sheath are normal in adduction, adduction is associated with abnormally great globe retraction in POAG without elevated IOP. Traction in adduction may cause mechanical overloading of the ON head and peripapillary sclera, thus contributing to or resulting from the optic neuropathy of glaucoma independent of IOP.

Keywords: biomechanics, orbit, extraocular muscle, magnetic resonance imaging

Glaucoma is the second leading cause of blindness worldwide,[1] and is more prevalent with increasing age. The historic view has been that glaucoma is caused by elevated IOP that damages the optic nerve (ON). The Advanced Glaucoma Intervention Study demonstrated that IOP reduction within the normal range to between 18 and 14 mm Hg modestly, but significantly reduced progressive visual field (VF) loss over a 6-year interval.[2] Nevertheless, the etiologic role of IOP in the pathogenesis of glaucoma has been removed from the definition of the disease for many reasons, including observations that many patients with glaucoma, especially in Asia,[3] lack abnormally high IOP and may sustain progressive ON damage at statistically normal IOP. Non–IOP-dependent causes of glaucomatous ON damage have been suggested to include vasospasm[4] or translaminar gradients against intracranial pressure (ICP) as causes of ON damage,[5–8] but a clear etiology for primary open-angle glaucoma (POAG) with or without elevated IOP has not emerged.

Patients with POAG who suffer glaucomatous ON damage at normal IOP levels have been considered by some to have normal tension glaucoma (NTG).[9] While others dispute the value of NTG as a diagnostic entity,[9] it is generally accepted that a subgroup of patients with POAG suffer significant ON damage without evidence of IOP elevated above the statistical range of normal IOPs recorded in population-based surveys,[10] and the term is now so widespread in the published literature that there were over 2000 citations of it in PubMed by mid-2017. Notwithstanding that IOP reduction may slow the glaucomatous process in some of these patients,[11–13] there clearly must exist an IOP-independent mechanism of progressive optic neuropathy unresponsive to IOP reduction to any level.[10,14]

The historic concept of glaucoma pathogenesis as mechanical damage to the ON head resulting from excessive IOP force pushing from within the eye has been challenged recently by the proposal that similar damage could arise from force pulling from outside the eye.[15,16] Tractional force is well known to be

harmful to nerves, with only 6% stretch markedly altering electrophysiological properties in peripheral nerves[17] and 8% strain fully blocking brachial plexus conduction.[18] Magnetic resonance imaging (MRI) has demonstrated that the ON and its surrounding sheath are insufficiently long to permit unhindered adduction in healthy people, becoming taut beyond approximately 20° of adduction and tethering the globe.[15] Optical coherence tomography (OCT) has demonstrated progressive deformation of the normal ON head and peripapillary sclera in adduction,[19] and in both adduction and abduction.[20] Although even abduction deforms the ON head modestly, these dynamic imaging studies imply that the ON sheath applies a mechanical load onto the globe in adduction, opposing the adducting force exerted by the medial rectus (MR) extraocular muscle. Consistent with Newton's third law of motion, every force acting on the eye is opposed by an equal reaction force or sum of reaction forces. In large angle adduction, MR force is not simply opposed by lateral rectus (LR) force but also by the reaction force exerted by stretching the ON and its sheath. Moreover, while the powerful MR's force is applied across a broad tendon insertion,[21] the equal reaction force is concentrated on a very small area at the temporal edge of the ON canal, so that local stress (force divided by area) there is commensurately much higher. Resulting mechanical deformation in this region might damage the lamina cribrosa (LC) and peripapillary sclera, critical tissues damaged in glaucoma. Sibony et al.[22] have suggested that ocular motor forces may contribute to peripapillary subretinal hemorrhage. In cases of axial high myopia, MRI demonstrates that adduction tethering by the ON can retract the globe.[15] The patterns of mechanical strain in the posterior sclera predicted to result from ON tethering[23] closely match the temporal peripapillary atrophy typical of NTG[24–26] and the peripapillary staphylomata typical of axial high myopia.[27] While Wang et al.[16] predicted, based on finite element analysis, that horizontal eye movements would strain the peripapillary region, their analysis also predicted a greater effect in adduction than in abduction.

We investigated a possible tractional cause of glaucomatous optic neuropathy by using multipositional MRI to study patients with POAG who exhibit characteristic VF loss and have glaucomatous structural ON and nerve fiber layer damage without evidence of elevated IOP. If hypothesized ON traction were an IOP-independent pathogenic factor in optic neuropathy, we predicted that MRI would demonstrate greater globe dislocation from ON tethering in adduction than in control subjects who do not have POAG.

Methods

Subjects

This study was prospectively approved by the institutional review board for Protection of Human Subjects of the University of California, Los Angeles, and conformed to the tents of the Declaration of Helsinki. Subjects gave written informed consent prior to participation. From a large multiphysician, academic glaucoma practice, 17 patients were recruited who had been diagnosed and treated for POAG and were considered to have NTG with the following inclusion characteristics: applanation IOP never recorded to exceed 21 mm Hg, with or without medical or surgical treatment, on multiple clinical examinations and ophthalmoscopic examinations, and OCT evidence of ON disc features and nerve fiber layer loss that correlated with typical glaucomatous VF defects on Humphry automated perimetry. Ophthalmoscopic features of glaucoma included disc hemorrhages,[28] but neither these nor a defined cup-to-disc ratio were required, consistent with modern clinical practice. Patients were excluded if they had previously undergone incisional ocular surgeries besides those for cataract, glaucoma, or refractive error, or if they had any other cause for optic neuropathy or VF defects besides glaucoma. Medical records of subjects with POAG always included multiple IOP measurements on multiple examination days, ON photos, OCT examinations of the ON, and standard automated perimetry examinations (with programs 24-2 or 30-2) performed within 1 year of recruitment. Glaucoma specialists according to best practices were actively managing all subjects at the time of the study.

A control group was recruited by advertising from the community and from patients followed in a comprehensive practice for refractive error without suspicion of glaucoma or optic neuropathy. Control subjects were required to have best corrected visual acuity of 20/20 in each eye, normal IOP by applanation, and were excluded if they had previously undergone ocular surgeries besides those for cataract or refractive error, had significant prior ocular trauma, or if they had any other ocular disorder except for refractive error or lens opacity. Control subjects underwent ophthalmic examination by the senior author to verify eligibility.

MRI Acquisition

The senior author performed high-resolution MRI of the orbits with a 1.5T General Electric Signa scanner equipped with a custom, dual-channel array of surface coils embedded in a facemask (Medical Advances, Milwaukee, WI, USA). Eye position was controlled by instructing subjects to visually fixate a fine, illuminated fiber optic target presented monocularly in a central position or in a lateral position selected to establish abduction. Because the nose or surface coil occlude viewing by the adducting eye, imaging in adduction was performed during abducted fixation by the fellow eye. General aspects of the high-resolution orbital MRI were as published.[29–33] A T2 fast spin echo pulse sequence was employed to obtain high tissue contrast with minimum acquisition time[29]; this sequence distinguishes the ON from its sheath by the bright ring of cerebrospinal fluid between the two (Fig. 1, right). A triplane localizer scan was performed to guide subsequent imaging. In most cases, an axial set of 12 contiguous, 2-mm thick MRI planes (field of view 10×10 cm, 256×256 matrix) that included both orbits was obtained to verify the gaze directions for each fixation direction, and to determine globe axial length (AL) and ON length in gaze positions where the ON was straight. Axial acquisition for each gaze direction was followed by contiguous, quasicoronal 17 to 20 sets of 2-mm thick planes perpendicular to the long axis of each orbit separately (field of view 8×8 cm, 256×256 matrix, resolution 312 μm in plane). These acquisitions were repeated for central gaze, as well as large (~30°), or both moderate (~15°) and large abduction and adduction of each eye (Fig. 1). Image quality and gaze direction were evaluated by an investigator online after every acquisition during the scanning sequence, although quantitative analysis was performed later offline.

MRI Analysis

MRI Analysis was performed with ImageJ 64 software (http://imagej.nih.gov/ij/; provided in the public domain by the National Institutes of Health, Bethesda, MD, USA) and custom algorithms written in Excel (Microsoft, Redmond, WA, USA). The gaze direction of each eye was computed in axial images (Fig. 1, left) as the angle of a line connecting the perpendicular of its lens plane with its fovea, after first rotating the entire image to orient the midsagittal line vertically.[31] While this

Investigative Ophthalmology & Visual Science

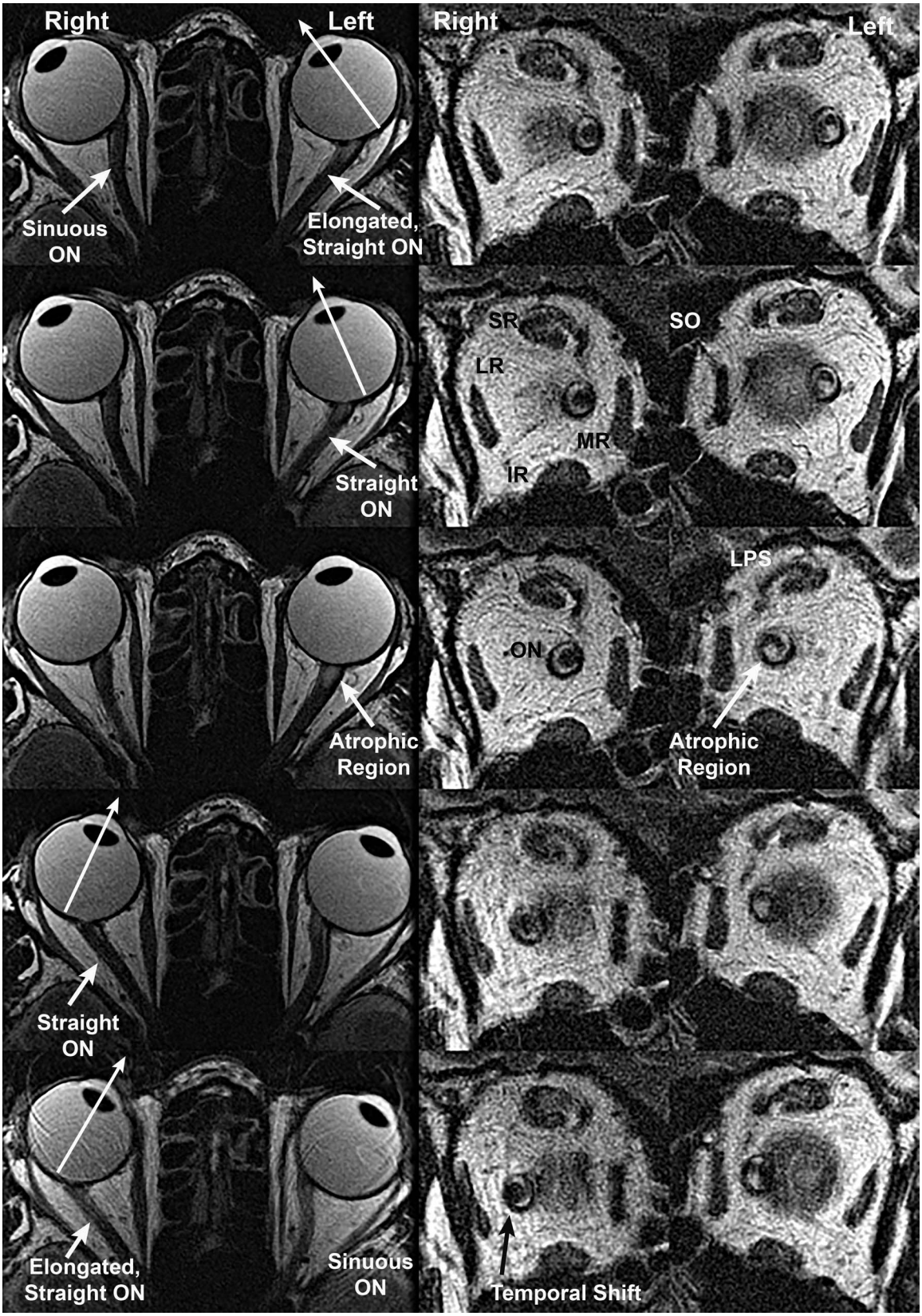

Figure 1. Axial (*left column*) and quasicoronal (*right column*) MRI of both orbits in a patient with advanced POAG with IOP never exceeding the normal range, imaged in maximal dextorversion (*top row*), moderate dextroversion (*second row*), cental gaze (*center row*), moderate levoversion (*fourth row*), and maximal levoversion (*bottom row*). The optic nerve (ON) of each eye straightened in moderate adduction and remained straight in maximal adduction, while it was sinuous in abduction. Coronal views taken just posterior to the globe-ON junction demonstrate that the ON within its sheath is surrounded by a bright ring of cerebrospinal fluid, but the ON shifts to the temporal side of the sheath in adduction. Both ON cross sections are subnormal due to glaucomatous atrophy, but a focal area of atrophy is also evident in the inferior ON cross section of the left eye. IR, inferior rectus muscle; LPS, levator palpebrae superioris muscle; LR, lateral rectus muscle; MR, medial rectus muscle; SR, superior rectus muscles.

Investigative Ophthalmology & Visual Science

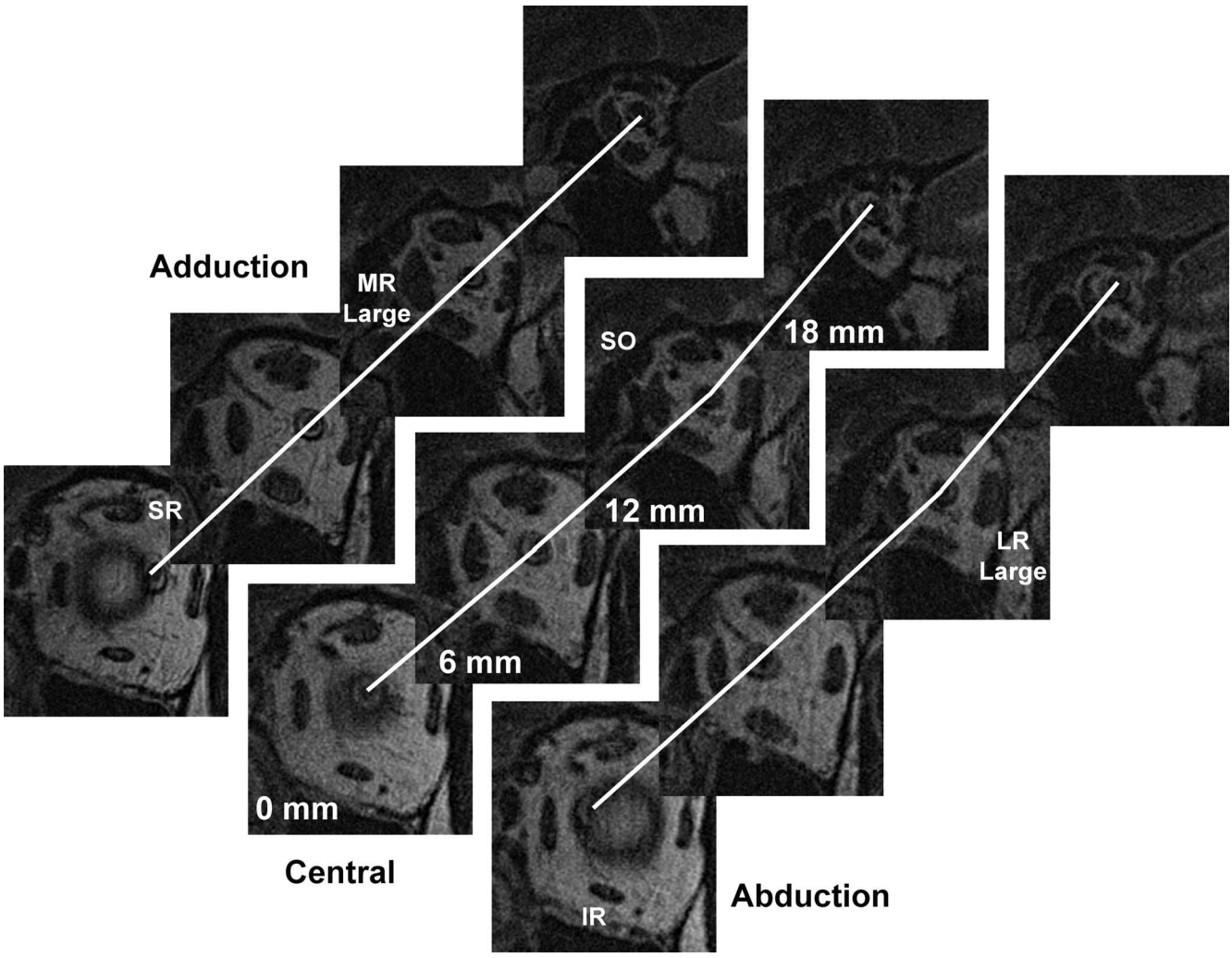

Figure 2. Quasicoronal MRI of left orbit of patient with POAG and IOP not exceeding 21 mm Hg, repeated in adduction, central gaze, and abduction, shown in planes at 6-mm intervals posteriorly from the globe-ON junction. Lines interconnect optic nerve centroid, showing a straight ON path only in adduction. Quantitative analysis was performed for ON path distances between each adjacent pair of 2-mm thick image planes, although inclusion of the omitted two planes between each of the illustrated planes would show further sinuosity in central gaze and abduction.

objective approach does not account for angle kappa or other discrepacies between the anatomic angle and subjective visual direction, it is reliable for determination of changes in gaze angle.[31]

Contiguous, quasicoronal MRI images were used to generate an independent, quantitative measure of ON path length and straightness of the ON and its sheath in three-dimensions (3D) (Fig. 1 right, and Fig. 2); this measure was employed for all gaze directions. The ON and sheath, where separately disinguishable, were manually outlined in each image plane in which they appeared. Then the ImageJ 64 software computed horizontal and vertical coordinates of the area centroid, with the third dimension corresponding to the incremental anteroposterior coordinate of each 2-mm thick image plane (Fig. 2). Use of area centroids, which are determined from multiple contiguous pixels, permits measurement at resolution finer than the size of a pixel. Cartesian distances between centroids in each adjacent pair of image planes were summed using custom algorithms to compute the overall path lengths for the ON and ON sheath as well as for selected nasal and temporal portions of the ON sheath. Minimum geometric distances between the globe-ON junction and the most posterior image plane in which the ON was visible were computed from Cartesian distances between the 3D coordinates of these two points. The ratio between actual ON path length and the minimum path length between the globe and the most posterior point imaged, represented in percent, was taken as a measure of straightness, with 100% being the theoretical minimum for a straight path determined without any image or measurement "noise."

Equatorial globe diameter was determined at subpixel resolution from cross sections in three quasicoronal image planes spanning the equator.[34] Globe AL was measured directly from the anterior corneal surface to the retinal surface in the axial MRI plane that included maximum globe diameter, and was averaged for each eye over measurements in all gaze positions imaged (typically 3–5 duplicates). Equatorial globe diameter was available for all subjects, but AL data was available only for subjects in whom high-resolution axial MRI was performed.

Gaze direction was independently determined from changes in the location of the globe-ON junction in quasicoronal images (Fig. 1, right), as previously described.[34] The 3D location of the globe center were determined at subpixel resolution from outlines of globe cross sections in multiple quasicoronal planes referenced to the centroid of the orbit.[34] This method is robust and has been extensively used in MRI studies of extraocular muscle paths and pulley positions in relation to the globe

Table 1. Large Ductions Achieved During Magnetic Resonance Imaging

		Abduction - Degrees				Adduction - Degrees			
		Horizontal		Vertical		Horizontal		Vertical	
Group	*N* Orbits	Mean	SEM	Mean	SEM	Mean	SD	Mean	SEM
POAG with normal IOP	34	21.1	0.9	0.2	0.7	28.6	0.8	0.0	1.1
All controls	59	20.6	0.7	−.3	0.5	26.8	1.1	−1.5	0.7
Age-matched controls	19	21.6	1.4	−1.0	0.6	24.5	2.0	−1.4	1.3

Angles were computed from quasicoronal images. Supraduction is designated as positive. None of the differences in horizontal duction among groups was statistically significant ($P > 0.2$).

center.[34–37] All analytic steps subsequent to manual outlining of structures in the MRI images were automated.

Validity of determinations of ON straightness was confirmed independently by different investigators analyzing axial compared with quasicoronal images for the same subjects viewing the same targets, with one investigator assigned to each type of image at a different time and place. Robustness and validity of the quasicoronal analyses was confirmed by duplicate analyses at separate times by two different investigators of the image sets of 10 representative subjects.

Initial statistical analyses were performed using *t*-tests using GraphPad Prism software (GraphPad Software, LaJolla, CA, USA). Differences in results obtained using individual eyes as the unit of sampling that appeared significant were then confirmed using generalized estimating equations (GEE) in SPSS software (IBM Corporation, Armonk, NY, USA); this approach, which can include multivariate analysis, avoids confounding by possible interocular correlations between the two eyes of individual subjects.

Results

Subject Characteristics

Included for analysis were 34 orbits of 17 patients who had POAG without elevated IOP; there were 11 women and 6 men of average (±SD) 62 ± 10 years. Average perimetric MD for the 30 eyes was –8.2 ± 1.2 dB. Analyzed as controls were 59 orbits of 32 healthy subjects; there were 13 women and 17 men of average age 37 ± 19 years. Because the full control group was significantly younger than the patients ($P = 0.0001$), we also analyzed an age-matched control subgroup of 19 orbits of 10 older healthy subjects of average age 63 ± 6 years ($P = 0.708$).

Ocular Hypotensive Treatments

All subjects with POAG were receiving bilateral treatment with topical medications, including prostaglandin synthase inhibitors latanoprost or brimatoprost in every subject. Four subjects were also treated with timolol, six with brimonidine, three with brinzolamide, and two with dorzolamide. Five eyes had undergone prior trabeculectomy, and 8 had undergone selective laser trabeculoplasty.

Globe Size

Equatorial globe diameter in patients with POAG averaged 25.95 ± 1.07 mm, significantly greater than the 25.24 ± 1.40-mm diameter in the full control group ($P = 0.041$, GEE), but not significantly different from the 25.64 ± 1.55-mm diameter in the age-matched controls ($P = 0.513$, GEE). Mean AL of patients with POAG averaged 25.60 ± 1.43 mm, not significantly different from the corresponding value (25.57 ± 1.60 mm, $P = 0.722$) for all control subjects in whom it was available.

Optic Nerve Straightness

In all patients and control subjects, the ON became straight in adduction, and was typically redundant in abduction, for example, as shown in the axial images in Figure 1 (left). However, apparent straightness in the axial plane does not exclude coexisting sinuosity perpendicular to the axial plane. To verify ON path straightness in 3D, sets of contiguous, 2-mm thick quasicoronal images were analyzed to compute the summed distances between adjacent ON area centroids. Figure 1 (right) illustrates for one patient the quasicoronal image plane immediately posterior to the junction of the globe and optic nerve, but images parallel to this one (Fig. 2) were obtained every 2-mm posteriorly to the orbital apex.

All subjects in the study underwent MRI in central gaze and large angles of abduction and adduction. Large duction angles achieved are summarized in Table 1. Abduction did not vary significantly from approximately 21° for all groups ($P > 0.2$), nor did adduction vary significantly from 24° to 29° for all groups ($P > 0.1$, Table 1). Subjects with POAG had no significant associated vertical duction associated with horizontal duction ($P > 0.85$), although there was statistically significant infraduction of less than 2° in the full ($P < 0.02$) and age-matched ($P < 0.05$) control subject groups for both abduction and adduction. While this infraduction is statistically significant given the large sample size with small measurement variability, it is probably not physiologically important and it is unlikely that the measures of ON straightness reported below were significantly confounded by differences in eye position.

Quantitative measures of ON straightness were obtained from 3D path lengths determined from ON centroid positions in sets of adjacent quasicoronal MRI planes (Fig. 2). While such image sets do not include the entire ON path, from them it is possible to compare the actual path of the ON centroid with the shortest, straight line distance in 3D from the globe-ON junction to the most posterior part of the ON imaged in each set. Such data represent ON path as a percentage of minimum path distance and can be no less than 100%. Figure 3 shows ON path straightness relative to shortest geometric distance to the globe-ON junction for the gaze positions listed in Table 1: central gaze, large angle abduction averaging 21° to 22°, and large angle adduction averaging 24° to 28°. In all groups, the ON was significantly straighter in adduction than in the other gaze positions, and its straightness in adduction did not differ significantly among groups ($P > 0.15$, GEE). This minimum value of relative ON path length does not reach the theoretical nadir of 100%, because all image quantization artifacts and other analysis error tends to increase, but never decrease, measured path length. Therefore, it may be inferred that the ON was completely straight in large angle adduction in all subject groups. In all groups, ON path length was a highly significantly greater percentage of geometric minimum in central gaze and in abduction than in adduction ($P \leq 0.003$), reflecting redundancy of ON length. However, in central gaze ($P = 0.041$, GEE) and abduction ($P = 0.006$, GEE), the ON was

Investigative Ophthalmology & Visual Science

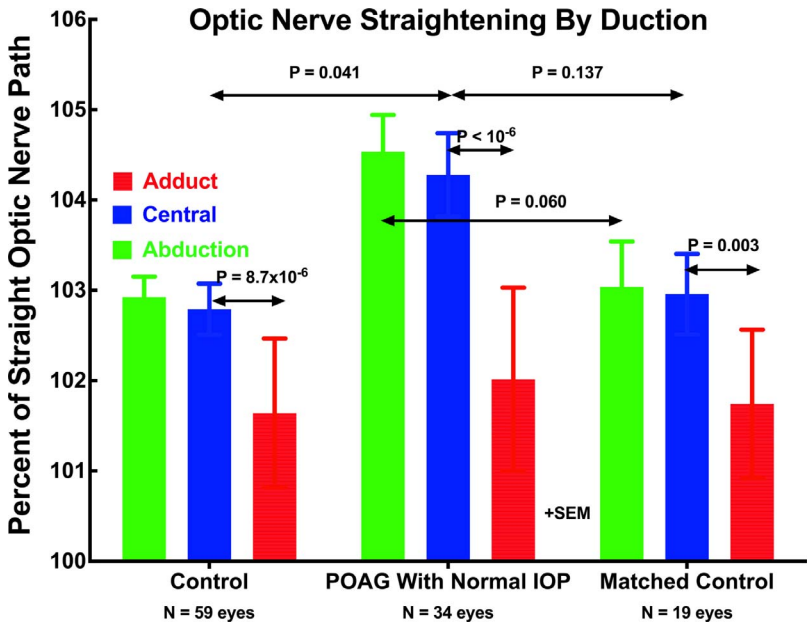

FIGURE 3. Optic nerve straightness represented as path length relative to shortest geometric distance to the globe-ON junction in central gaze, large angle abduction averaging 21° to 22°, and large angle adduction averaging 24° to 28°. In all groups, the ON was significantly straighter in adduction than in the other gaze positions, and its straightness in adduction did not differ significantly among groups ($P > 0.15$). However, in central gaze and abduction, the ON was significantly more redundant in POAG than in the full control group.

significantly more redundant in subjects with POAG than in the control groups.

In the group with POAG and normal IOP, the ON was significantly more redundant at approximately 104.5% of minimum in central gaze and abduction than in the full and matched control groups (Fig. 3). Because the ON was similarly straight in adduction in all groups, relatively more straightening occurred in the subjects with POAG than in the others.

Confirmation of Optic Nerve Straightness

Consecutive subgroups of subjects with POAG and controls were scanned in two angles of abduction and adduction for each eye, with differences in eye positions representing incremental changes in duction for target presentation to the abducting eye. In each case, the resulting smaller adduction of the fellow eye was estimated a priori to be sufficient to fully straighten its ON, and the increment was to the maximum position that the abducting eye could fixate as limited by either target visibility or the subject's ocular motor range. This permitted verification from quasicoronal images that the ON path was straight in both adduction positions based upon a low percentage of minimum path (Fig. 4).

Globe Translation

Translational changes in the 3D position of the globe center relative to its position in central gaze were evident in both large abduction and adduction (Fig. 5). Subjects with POAG had highly significantly greater posterior globe translation in adduction than did the control group ($P < 10^{-6}$ by t-test, $P = 0.000$ GEE) or age-matched control group ($P < 0.00002$ by t-

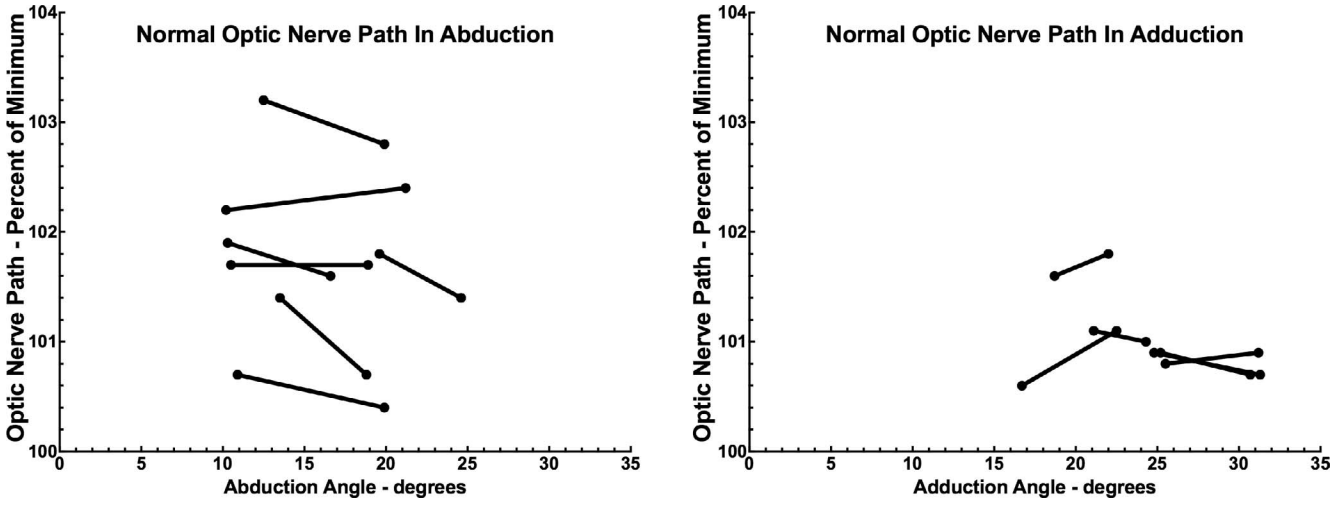

FIGURE 4. In controls, ON path length was near minimum in moderate and large adduction, but was generally much more redundant in abduction. This confirms ON straightness in the two incremental adducted positions connected for each subject by line segments.

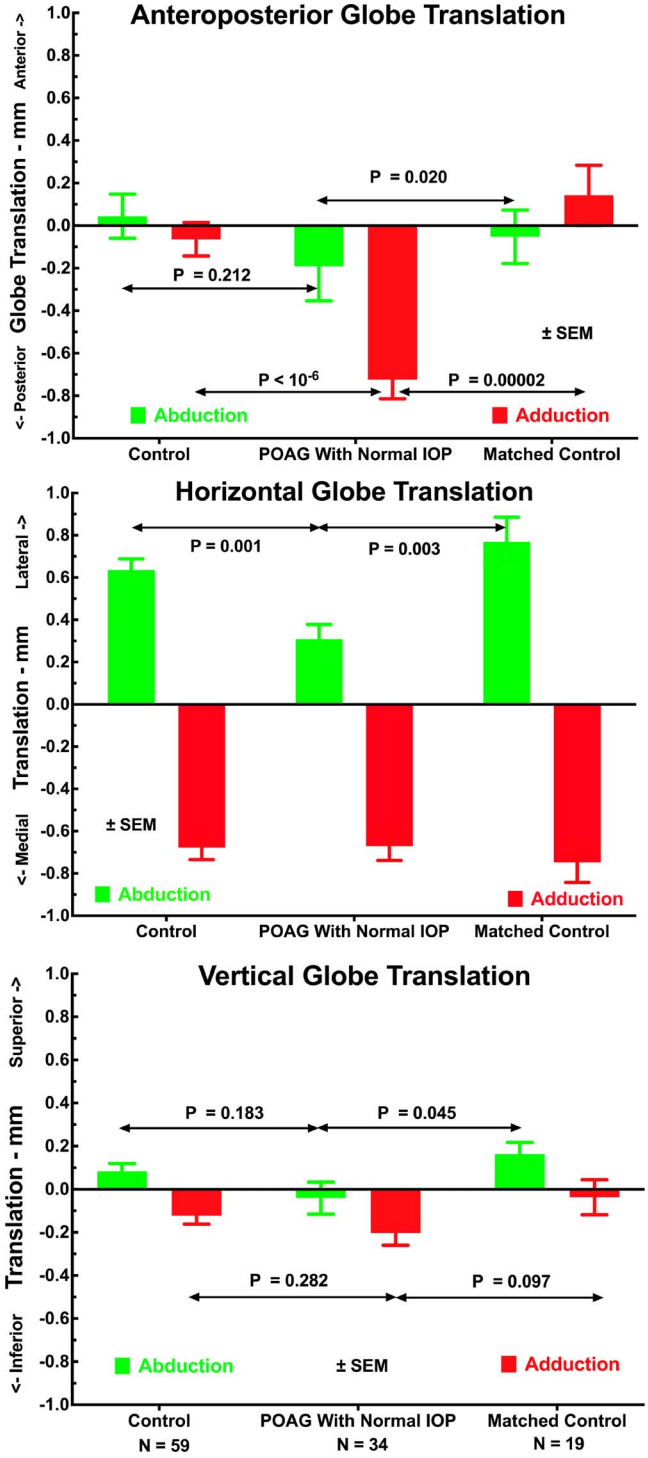

Figure 5. Effect of large duction on mean translation of the globe center relative to its position in central gaze for all control orbits, orbits having POAG with normal IOP, and the subset of control orbits matched in age to those of subjects with POAG. Orbits with POAG had significantly greater posterior and inferior globe translation in adduction than did the controls, yet significantly less lateral translation in abduction. There were no significant differences among groups in vertical globe translation in adduction.

test, $P = 0.000$ GEE, Fig. 5, top). Subjects with POAG and both control groups exhibited similar medial globe translation in adduction of about 0.7 to 0.8 mm (Fig. 5 center, $P > 0.5$). All groups exhibited lateral globe translation in abduction, although this was significantly less at approximately 0.3 mm for the group with POAG than for both control groups at about 0.6 mm ($P < 0.003$, Fig. 5, center). Vertical globe translation during horizontal duction was less than 0.3 mm for all groups, with no major differences among groups except for slightly greater superior globe translation in adduction in the older control group than in the group with POAG ($P = 0.045$).

Table 2. Generalized Estimated Significance Levels of Effects of POAG Without Elevated Intraocular Pressure on Globe Translation During Horizontal Gaze

Translation Direction	Abduction	Adduction
Anteroposterior	0.040	0.004*
Horizontal	0.027	0.203
Vertical	0.203	0.693

Significance levels of Wald χ^2 tests of GEE linear model fits of globe translation with horizontal gaze, with models incorporating presence or absence of POAG, sex, equatorial globe diameter, and age, corrected for possible correlations between the paired eyes of individual subjects. The most significant model effect was that of adduction on anteroposterior globe translation.

* Retraction.

Effects of Age, Sex, and Globe Diameter on Globe Retraction in Adduction

Data on anterior globe translation in adduction from all subjects in all groups was pooled and subjected to multivariate analysis using GEE (Table 2). These data, with simple linear fits to age and equatorial globe diameter, are plotted in Figure 6. Subject age and coronal plane globe diameter both had highly significant effects for all directions of globe translation in abduction and adduction ($P = 0.000$, GEE). Beyond this, the presence of POAG without elevated IOP was also significantly related to posterior globe translation in adduction ($P = 0.004$) and abduction ($P = 0.04$), but not horizontal or vertical translation in adduction, or vertical globe translation in abduction. There was no significant effect of subject sex on any measure of globe translation with gaze ($P = 0.8$).

Discussion

The present axial and coronal plane MRI study confirms a 1941 geometrical deduction by Friedman[38] and quantitatively extends the twenty-first century MRI report of Demer that, while the ON is redundant in central gaze and abduction, it becomes taut in adduction where it tethers and exerts traction on the globe.[15] Beyond the threshold of straightening in adduction, the ON and sheath can only stretch while following a straight path.

Tethering of the ON tethering in adduction has several consequences. First, when the eye continues to adduct past the point at which the ON has exhausted redundancy and becomes straight, the ON and its surrounding sheath, as well as the globe and associated orbital tissues, must inevitably stretch, or stretch and change their anatomic configurations. While ON tethering in adduction appears to occur in nearly everyone, MRI shows here that patients who have POAG without history of elevated IOP have significantly greater ON redundancy in central gaze and abduction than control subjects (Fig. 3). The greater ON redundancy of patients with POAG in central gaze does not confer protection from ON tethering in adduction, because MRI demonstrated that ON tethering occurred nonetheless. Moreover, in POAG the tension in the ON and its sheath in adduction was associated with abnormal globe

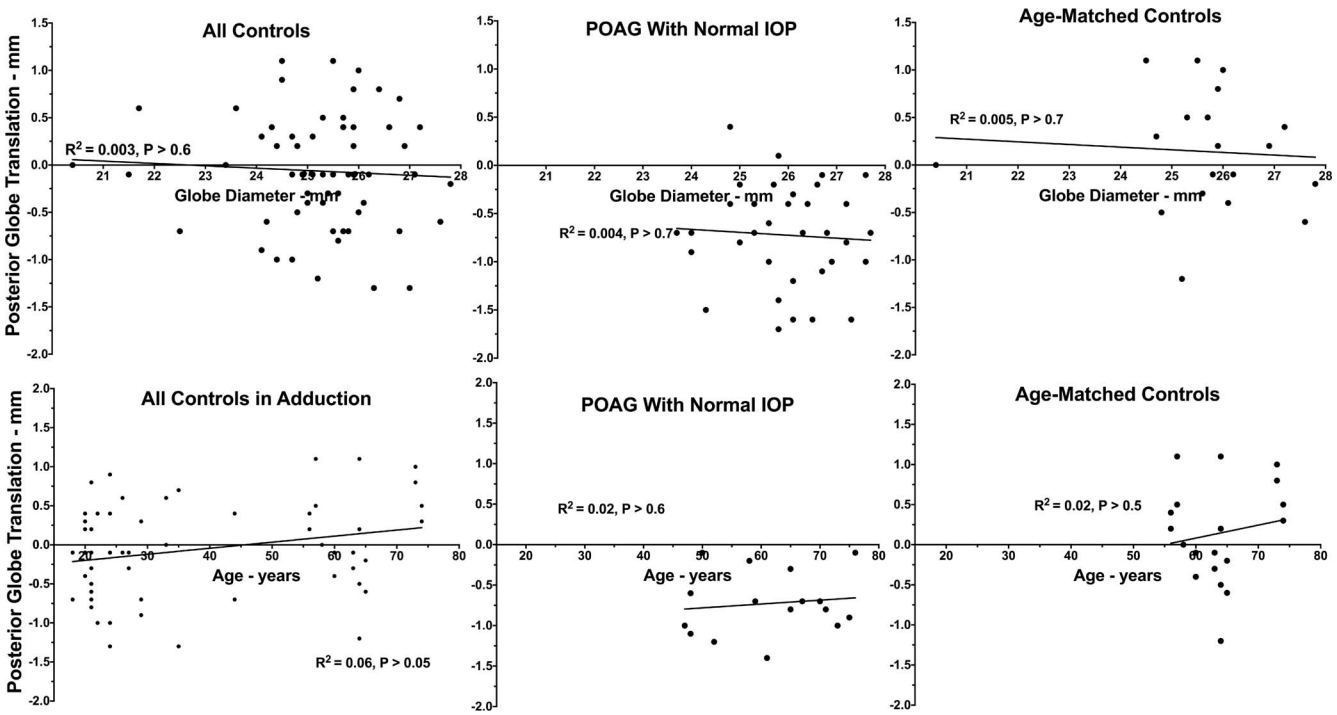

Figure 6. Posterior globe translation as a function of equatorial globe diameter (*top*) and subject age (*bottom*) for all subject groups, with simple linear regression fits. Coefficients of determination R^2 were low for both globe diameter and age, although GEE analysis demonstrated significant effects of both in Table 1.

displacement. In both patients with POAG and controls, the entire globe translated medially in adduction by 0.7 to 0.8 mm (Fig. 5, center); in controls, the entire globe translated laterally in abduction by about that same distance, but lateral globe translation in abduction was less than half that in POAG. Importantly, in POAG but not in overall control or age-matched control subjects, ON tethering in adduction was associated with highly statistically significant globe retraction of approximately 0.7 mm (Fig. 5, top). This effect was significant even after consideration of the separate, also significant effects of subject age and horizontal globe diameter. Thus, only in POAG without elevated IOP, abnormal globe retraction occurs as the ON tethers the globe in large adduction.

In biomechanical terms, globe translation can be interpreted as mechanical strain on the orbital suspensory tissues. Presumably, when the ON and sheath of healthy people become tethered in adduction, these structures stretch more freely to reduce globe deformation and translation, thus absorbing the strain. In POAG without elevated IOP, we infer that the ON and sheath are abnormally stiff, and stretch less freely during adduction tethering, thus transferring the associated strain to the globe at the vulnerable peripapillary junction. During adduction in POAG, the stiff ON and sheath shift the entire globe posteriorly. Given anatomic considerations, it seems likely that the bulk of the tethering force in adduction is exerted by the stiff ON sheath (Shin A, et al. *IOVS* 2017;58:ARVO E-Abstract 3160), whose collagen is dense and whose elastin fibrils are woven in crisscross orientations for high, uniform mechanical strength (Le A, et al. *IOVS* 2017;58:ARVO E-Abstract.1736). The ON sheath's inner layer inserts on the sclera closest to the lamina cribrosa (Baig A, et al. *IOVS* 2017;58:ARVO E-Abstract 1738). Biomechanical properties of sclera and lamina cribrosa may contribute to ON axonal damage, and thus to glaucoma,[39] as reviewed.[40,41] Strain in the lamina cribrosa is so strongly influenced by the sclera[41–43] that the normal range of variation in peripapillary scleral thickness is estimated to have an effect similar to an IOP change of 15 mm Hg.[44] Peripapillary sclera is subject to variation in nonlinearly viscoelastic properties that depend on loading rates and directions[41] relevant for transient mechanical behavior during eye movements.[40]

The foregoing functional anatomic effects of adduction tethering by the ON and its sheath have multiple clinical correlates. Purkinje in the nineteenth, Helmholtz in the early twentieth, and Enoch et al.[45] in the early twenty-first, centuries described gaze-evoked phosphenes adjacent the physiologic cecum.[46] Purkinje, Helmholtz, and Friedman reported greater prominence of such phosphenes with adduction and convergence than with abduction.[38,46] Using a mechanical model, Enoch et al.[45] inferred that ocular duction could deform the posterior globe, a prediction supported by finite element biomechanical analysis suggesting that ONH strain could arise from horizontal duction and exceed that caused by marked IOP elevation.[16,47] Sibony[48] and Chang et al.[19] demonstrated by OCT that the peripapillary Bruch's membrane of healthy subjects is deformed by horizontal duction, and Sibony further observed that this deformation is reversibly exaggerated in papilledema. Wang et al.[20] demonstrated by OCT that strain in the human lamina cribrosa is associated with horizontal eye movement. All of these observations are consistent with the present MRI demonstration of ON and sheath traction on the temporal peripapillary region in adduction. Moreover, the entoptic phenomena in adduction lack a plausible alternative explanation because they persist after posterior vitreous detachment.[45] While readily demonstrable in fields of view limited to approximately 10 mm using axial plane OCT, adduction-related peripapillary distortion is below the threshold of detection by MRI as performed here.

The present study demonstrates abnormal adduction-tethered globe retraction in subjects who have POAG without elevated IOP; while these findings are absent in subjects without POAG, causality is not established merely by demon-

stration of the association. The possibility of a causal relationship to glaucomatous optic neuropathy should be considered in the context, among other things, of biological plausibility. First, does large adduction occur frequently enough to constitute a potentially damaging mechanism? The human horizontal oculomotor range of approximately ±55°[49] is about double the adduction achieved by subjects during the MRI scans in the current study, so the current range of eye movements can certainly be considered physiologic. Approximately three saccades occur every second,[50] equivalent to approximately 183,000 saccades daily,[51] including those during rapid eye movement sleep.[52] At least in healthy subjects, convergence to near targets is not associated with globe retraction; in fact the opposite occurs, with MRI demonstrating proptosis of 0.5 mm during 22° asymmetrical convergence.[31] Scanning saccades during reading probably does not load the ON as much as the largest and fastest adduction that occurs during ocular tracking, or during natural head rotations. The vestibulo-ocular reflex (VOR) generates automatic ocular counter-rotations during head movement, particularly during active head rotation. Slow phases of the VOR alternate with saccade-like quick phases. Importantly, the VOR is coordinated with large saccades during head rotations that achieve the large gaze shifts required during walking, running, and most natural activities of daily life. Large gaze saccades coordinated with head movement include eye movements averaging approximately 30°.[53,54] Subjects instructed to touch at arms' length a sequence of targets at tabletop level regularly make saccades as large as 40° to 45°.[55] Thus, the adductions sustained for several minutes during the current MRI study are probably only approximately half as large as transient saccades common in daily life.

The globe retraction associated with tethering by the ON in adduction directly visualized by MRI in the current study is not the only known mechanism that could cause anteroposterior globe translation in adduction. Agonist and antagonist extraocular muscles of the same eye normally contract and retract in reciprocal fashion so as to avoid cocontraction and consequent changes in total force that would retract the globe. However, extraocular muscle volume increases during contraction and decreases during relaxation; for this reason, total extraocular muscle volume in the normal orbit increases with adduction by an average of 32 μL (2.3%).[56] The change in muscle volume in adduction would therefore tend to shift the globe anteriorly, opposite the retraction observed here. The relatively rare congenital cranial dysinnervation disorders,[57] most prominently including Duane syndrome, often exhibit globe retraction in adduction due to cocontraction of the medial and lateral rectus muscles.[58] None of the subjects in this study had a congenital cranial dysinnervation disorder.

Peripapillary phosphenes occur during ordinary saccades, indicating that these saccades are mechanically sufficient to perturb the region of the ON head. Peak isometric tension in human horizontal rectus muscles averages 40 gram-force (gm-f) for a 20° saccade and 52 gm-f for a 30° saccade, while steady state tension after these saccades averages 26 and 33 gm-f, respectively.[59] These correspond to 0.25 to 0.5 N in metric units. For perspective, repetitive motion injury occurs when the bony wrist is extended 15 times per minute at 15 N force for 7 hours daily for 3 weeks.[60] Extraocular muscle force during saccades is concentrated focally on the relatively soft globe at a level sufficient to rotate it over much of its maximal range, with movement frequency and cumulative lifetime repetitions far exceeding other movements that cause repetitive motion injury. The speed of eye movements may also contribute to ON damage. Saccades propagate stress waves in the eye that are damped by the vitreous gel.[61] As the vitreous detaches during aging, vitreous damping may diminish, perhaps increasing stress on the ON head and peripapillary tissues during saccades.

Glaucoma becomes more prevalent with advancing age,[62,63] possibly corresponding to increased cumulative likelihood of mechanical strain on the ON and peripapillary tissues during eye movement. Beyond the accumulation of lifetime eye movements, other factors may predispose to ON damage. The present data suggest that the ON and sheath of patients with POAG are probably stiffer (less elastic) than normal because the normal traction in adduction produces greater than normal globe retraction in POAG. There is some evidence that the ON sheath may stiffen as a general feature of normal aging (Shin A, et al. *IOVS* 2017;58:ARVO E-Abstract 3160; Baig A, et al. *IOVS* 2017;58:ARVO E-Abstracts 1738), but this could be exaggerated in people susceptible to POAG with normal IOP. The ON sheath is much stiffer than the peripapillary sclera into which it inserts. The peripapillary sclera is the most compliant of all sclera (Shin A, et al. *IOVS* 2017;58:ARVO E-Abstract 3160), so ON sheath traction observe here that was sufficient to retract the entire eye would likely deform the peripapillary region. The foregoing begs the question of why eye movements do not produce eventual ON damage in everyone. The answer may be that they do, but at very different rates in different people. Age-related thinning of the retinal nerve fiber and ganglion cell layers is considered a normal phenomenon,[64] although in most healthy people this axon loss extrapolates to symptomatic visual loss only at ages greatly exceeding the usual human life span.[65] The current findings suggest that adduction-related strain on the ONH is likely to be the most damaging in people who, as they age, continue to make large and vigorous adductions after their ON sheaths have become particularly stiff (hardened) relative to their peripapillary sclera, thus abnormally straining the ON head and LC during thousands of eye movements daily.

Adduction tethering may also explain the occurrence of peripapillary atrophy in POAG not associated with elevated IOP.[66–68] The mechanical effects of adduction tethering are expected to be maximal at the temporal edge of the ON's scleral canal, where the relatively stiff inner layer (Baig A, et al. *IOVS* 2017;58:ARVO E-Abstract 1738) of the ON sheath inserts at the confluence of the lamina cribrosa and peripapillary sclera. Young children typically lack an ON cup, ON head tilting,[69] peripapillary atrophy, and axial myopia[70]; these features develop as people age,[71] especially in myopia.[72,73] Axial myopia is strongly associated with glaucoma,[62,74] staphyloma, and peripapillary atrophy,[71] particularly on the temporal side.[71,75] Peripapillary atrophy[76] is common with glaucoma[24–26,74] and progresses with it,[24,66,67,77,78] and furthermore progresses with age[6] and with myopia.[27,74] Moreover, peripapillary atrophy not only correlates with the pattern[79] and severity of optic neuropathy and VF loss in glaucoma,[67,68] but also with the amount and direction ("torsion") of ON head tilt, which in turn correlate with VF defects in POAG,[80,81] better with normal than with high IOP.[82] Perhaps ON tethering in adduction may be a cause of progressive optic disc torsion, and even of axial myopia itself.[20]

The possibility must be considered that some of the unique features of subjects with POAG observed here might result from glaucoma therapy. All of these subjects were patients treated bilaterally with topical prostaglandin analogue agents, drugs associated with adnexal fat atrophy,[83] particularly the preaponeurotic lid fat.[84] For example, patients treated unilaterally with brimatoprost unilaterally develop ipsilateral relative enophthalmos[85,86] associated with reversible atrophy of the orbital fat.[86] Were ON length to remain constant during development of atrophic enophthalmos, ON redundancy would increase. Had atrophic enophthalmos occurred in the subjects with POAG in this series, resulting ON path

redundancy might have protected the ON and globe from traction in adduction, yet the adductions achieved by these subjects were not only sufficient to straighten the ON, but also were associated with abnormally large globe retraction. Moreover, using techniques identical to the current MRI study in 60 orbits of 31 subjects who had esotropia but not glaucoma, we have observed supernormal central gaze ON path redundancy that is comparable to that observed here in subjects with POAG without elevated IOP, although the esotropic subjects exhibited little globe retraction in adduction (Clark and Demer, unpublished data, 2017). Because these esotropic subjects were not treated with prostaglandin analogues, the finding in them of similar ON path redundancy shows that increased ON redundancy in central gaze does not require topical prostaglandin analogue therapy. Thus, it is likely that globe retraction during adduction tethering is a finding specific to POAG itself, not merely secondary to medical therapy for POAG.

If adduction tethering is indeed a major IOP-independent contributor to ON damage in POAG, therapeutic possibilities beyond IOP reduction become possible, but will require future study.

Study Limitations

As a cross-sectional comparison between patients with POAG who lack elevated IOP versus younger and age-matched control subjects who do not have glaucoma, this study could potentially have been subject to unknown confounds perhaps avoidable in a longitudinal study. The study did not address possible effects of ethnicity. Because the current study did not include a group of patients with POAG who do have elevated IOP, it provides no direct evidence of any possible contribution of ON tethering to optic neuropathy when the IOP is concurrently elevated. There is no reason in principle why both elevated IOP and ON tethering could not jointly act to produce glaucomatous neuropathy in patients simultaneously affected. The present study was mainly of patients who already had moderately advanced anatomic and visual field evidence of optic neuropathy; the study did not sufficiently sample a large range of POAG severity that might correlate with variations in the functional anatomy of the ON and orbital tissues. Moreover, even such correlations cannot demonstrate causality, or exclude the possibility that the present MRI findings might be the result rather than a cause of POAG. Conceivably, remodeling of an ON damaged by POAG might lead to replacement of axons by connective tissue, resulting in hardening of the ON and even its sheath as effects rather than causes of optic neuropathy. Such a hypothetic possibility could be excluded only by a long-term, prospective study. In the future, it would be desirable to study the effects of ON tethering in patients with POAG who have high versus normal IOP, and who have early versus advanced ON damage, and ultimately to do so longitudinally in the same individuals. It would also be desirable to obtain data on changes in the absolute length of the ON sheath to infer actual strain.

Acknowledgments

Presented at the annual meeting of the Association for Research in Vision and Ophthalmology, Baltimore, MD, USA, May 9, 2017.

Supported by grants from the US Public Health Service, National Eye Institute: Grants EY008313 and EY000331 (Bethesda, MD, USA); and by an Unrestricted Grant from Research to Prevent Blindness (New York, NY, USA). J.L. Demer is the Arthur L. Rosenbaum Professor of Pediatric Ophthalmology.

Disclosure: **J.L. Demer**, None; **R.A. Clark**, Nevakar, LLC (C); **S.Y. Suh**, None; **J.A. Giaconi**, None; **K. Nouri-Mahdavi**, None; **S.K. Law**, None; **L. Bonelli**, None; **A.L. Coleman**, None; **J. Caprioli**, None

References

1. Kingman S. Glaucoma is second leading cause of blindness globally. *Bull World Health Organ*. 2004;82:887–888.
2. The AGIS Investigators. The Advanced Glaucoma Intervention Study (AGIS): 7. The relationship between control of intraocular pressure and visual field deterioration. *Am J Ophthalmol*. 2000;130:429–440.
3. Shi D, Funayama T, Mashima Y, et al. Association of HK2 and NCK2 with normal tension glaucoma in the Japanese population. *PLoS One*. 2013;8:e54115.
4. Gramer G, Weber BH, Gramer E. Migraine and vasospasm in glaucoma: age-related evaluation of 2027 patients with glaucoma or ocular hypertension. *Invest Ophthalmol Vis Sci*. 2015;56:7999–8007.
5. Siaudvytyte L, Januleviciene I, Ragauskas A, et al. Update in intracranial pressure evaluation methods and translaminar pressure gradient role in glaucoma. *Acta Ophthalmol Scand*. 2015;93:9–15.
6. Jonas JB, Yang D, Wang N. Intracranial pressure and glaucoma. J Glaucoma. 2013;22(Suppl 5):S13–S14.
7. Berdahl JP, Fautsch MP, Stinnett SS, Allingham RR. Intracranial pressure in primary open angle glaucoma, normal tension glaucoma, and ocular hypertension: a case-control study. *Invest Ophthalmol Vis Sci*. 2008;49:5412–5418.
8. Berdahl JP, Allingham RR. Intracranial pressure and glaucoma. *Curr Opin Ophthalmol*. 2010;21:106–111.
9. Mi XS, Yuan TF, So KF. The current research status of normal tension glaucoma. *Clin Interv Aging*. 2014;9:1563–1571.
10. Song BJ, Caprioli J. New directions in the treatment of normal tension glaucoma. *Indian J Ophthalmol*. 2014;62:529–537.
11. Caprioli J. The treatment of normal-tension glaucoma. *Am J Ophthalmol*. 1998;126:578–581.
12. Collaborative Normal-Tension Glaucoma Study Group. The effectiveness of intraocular pressure reduction in the treatment of normal-tension glaucoma. *Am J Ophthalmol*. 1998;126:498–505.
13. Collaborative Normal-Tension Glaucoma Study Group. Comparison of glaucomatous progression between untreated patients with normal-tension glaucoma and patients with therapeutically reduced intraocular pressures. *Am J Ophthalmol*. 1998;126:487–497.
14. Choi YJ, Kim M, Park KH, et al. The risk of newly developed visual impairment in treated normal-tension glaucoma: 10-year follow-up. *Acta Ophthalmol*. 2014;92:e644–e649.
15. Demer JL. Optic nerve sheath as a novel mechanical load on the globe in ocular duction. *Invest Ophthalmol Vis Sci*. 2016;57:1826–1838.
16. Wang X, Fisher LK, Milea D, et al. Predictions of optic nerve traction forces and peripapillary tissue stresses following horizontal eye movements. *Invest Ophthalmol Vis Sci*. 2017;58:2044–2053.
17. Kwan MK, Wall EJ, Massie J, Garfin SR. Strain, stress and stretch of peripheral nerve. Rabbit experiments in vitro and in vivo. *Acta Orthop Scand*. 1992;63:267–272.
18. Takai S, Dohno H, Watanabe Y, et al. In situ strain and stress of nerve conduction blocking in the brachial plexus. *J Orthop Res*. 2002;20:1311–1314.
19. Chang MY, Shin A, Park J, et al. Deformation of optic nerve head and peripapillary tissues by horizontal duction. *Am J Ophthalmol*. 2016;174:85–94.
20. Wang X, Beotra MR, Tun TA, et al. In vivo 3-dimensional strain mapping confirms large optic nerve head deformations

following horizontal eye movements. *Invest Ophthalmol Vis Sci*. 2016;57:5825–5833.

21. Apt L. An anatomical reevaluation of rectus muscle insertions. *Trans Am Ophthalmol Soc*. 1980;78:365–375.
22. Sibony P, Fourman S, Honkanen R, El Baba F. Asymptomatic peripapillary subretinal hemorrhage: A study of 10 cases. *J Neuroophthalmol*. 2008;28:114–119.
23. Shin A, Yoo L, Park C, Demer JL. Finite element biomechanics of optic nerve sheath traction in adduction. *J Biomed Eng*. In press.
24. Jonas JB, Martus P, Horn FK, et al. Predictive factors of the optic nerve head for development or progression of glaucomatous visual field loss. *Invest Ophthalmol Vis Sci*. 2004;45:2613–2618.
25. Xu L, Wang Y, Yang H, Jonas JB. Differences in parapapillary atrophy between glaucomatous and normal eyes: the Beijing Eye Study. *Am J Ophthalmol*. 2007;144:541–546.
26. Jonas JB, Nguyen XN, Gusek GC, Naumann GO. Parapapillary chorioretinal atrophy in normal and glaucoma eyes. I. Morphometric data. *Invest Ophthalmol Vis Sci*. 1989;30:908–918.
27. Nakazawa M, Kurotaki J, Ruike H. Longterm findings in peripapillary crescent formation in eyes with mild or moderate myopia. *Acta Ophthalmol*. 2008;86:626–629.
28. Budenz DL, Huecker JB, Gedde SJ, et al. Thirteen-year follow-up of optic disc hemorrhages in the ocular hypertension treatment study. *Am J Ophthalmol*. 2016;174:126–133.
29. Demer JL, Dusyanth A. T2 fast spin echo magnetic resonance imaging of extraocular muscles. *J AAPOS*. 2011;15:17–23.
30. Shin GS, Demer JL, Rosenbaum AL. High resolution dynamic magnetic resonance imaging in complicated strabismus. *J Pediatr Ophthalmol Strabismus*. 1996;33:282–290.
31. Demer JL, Kono R, Wright W. Magnetic resonance imaging of human extraocular muscles in convergence. *J Neurophysiol*. 2003;89:2072–2085.
32. Demer JL, Ortube MC, Engle EC, Thacker N. High resolution magnetic resonance imaging demonstrates abnormalities of motor nerves and extraocular muscles in patients with neuropathic strabismus. *J AAPOS*. 2006;10:135–142.
33. Demer JL, Clark RA. Magnetic resonance imaging demonstrates compartmental muscle mechanisms of human vertical fusional vergence. *J Neurophysiol*. 2015;113:2150–2163.
34. Clark RA, Miller JM, Demer JL. Three-dimensional location of human rectus pulleys by path inflections in secondary gaze positions. *Invest Ophthalmol Vis Sci*. 2000;41:3787–3797.
35. Kono R, Clark RA, Demer JL. Active pulleys: magnetic resonance imaging of rectus muscle paths in tertiary gazes. *Invest Ophthalmol Vis Sci*. 2002;43:2179–2188.
36. Clark RA, Demer JL. Magnetic resonance imaging of the effects of horizontal rectus extraocular muscle surgery on pulley and globe positions and stability. *Invest Ophthalmol Vis Sci*. 2006;47:188–194.
37. Suh SY, Le A, Clark RA, Demer JL. Rectus pulley displacements without abnormal oblique contractility explain strabismus in superior oblique palsy. *Ophthalmology*. 2016;123:1222–1231.
38. Friedman B. Mechanics of optic nerve traction on the retina during ocular rotation with special reference to retinal detachment. *Arch Ophthalmol*. 1941;25:564–575.
39. Burgoyne CF, Downs JC, Bellezza AJ, et al. The optic nerve head as a biomechanical structure: a new paradigm for understanding the role of IOP-related stress and strain in the pathophysiology of glaucomatous optic nerve head damage. *Prog Retin Eye Res*. 2005;24:39–73.
40. Sigal IA, Ethier CR. Biomechanics of the optic nerve head. *Exp Eye Res*. 2009;88:799–807.
41. Downs JC. Optic nerve head biomechanics in aging and disease. *Exp Eye Res*. 2015;133:19–29.
42. Girard MJ, Downs JC, Burgoyne CF, Suh JK. Peripapillary and posterior scleral mechanics–part I: development of an anisotropic hyperelastic constitutive model. *J Biomech Eng*. 2009;131:051011.
43. Sigal IA, Flanagan JG, Tertinegg I, Ethier CR. Finite element modeling of optic nerve head biomechanics. *Invest Ophthalmol Vis Sci*. 2004;45:4378–4387.
44. Norman RE, Flanagan JG, Sigal IA, et al. Finite element modeling of the human sclera: influence on optic nerve head biomechanics and connections with glaucoma. *Exp Eye Res*. 2011;93:4–12.
45. Enoch JM, Choi SS, Kono M, et al. Utilization of eye-movement phosphenes to help understand transient strains at the optic disc and nerve in myopia. *Ophth Physiol Opt*. 2003;23:377–381.
46. von Helmholtz H. *Helmholtz's Treatise on Physiological Optics*. Washington D.C.: The Optical Society of America; 1924.
47. Wang X, Rumpel H, Lim WE, et al. Finite element analysis predicts large optic nerve strains heads during horizontal eye movements. *Invest Ophthalmol Vis Sci*. 2016;57:2452–262.
48. Sibony PA. Gaze-evoked deformations of the peripapillary retina and papilledema and ischemic optic neuropathy. *Invest Ophtalmol Vis Sci*. 2016;57:4979–4987.
49. Guitton D, Volle M. Gaze control in humans: eye-head coordination during orienting movements to targets within and beyond the oculomotor range. *J Neurophysiol*. 1987;58:427–459.
50. Wu CC, Kowler E. Timing of saccadic eye movements during visual search for multiple targets. *J Vis*. 2013;13(11):11.
51. Robinson DA. Control of eye movements. In: Brooks VB, ed. *The Nervous System, Handbook of Physiology*. Baltimore, MD: Williams & Wilkins; 1981:1275–1320.
52. Leclair-Visonneau L, Oudiette D, Gaymard B, et al. Do the eyes scan dream images during rapid eye movement sleep? Evidence from the rapid eye movement sleep behaviour disorder model. *Brain*. 2010;133:1737–1746.
53. Tomlinson RD, Bahra PS. Combined eye-head gaze shifts in the primate. II. Interaction between saccades and the vestibuloocular reflex. *J Neurophysiol*. 1986;56:1558–1570.
54. Tomlinson RD, Bahra PS. Combined eye-head gaze shifts in the primate. I. Metrics. *J Neurophysiol*. 1986;56:1542–1557.
55. Epelboim J, Steinman RM, Kowler E, et al. Gaze-shift dynamics in two kinds of sequential looking tasks. *Vision Res*. 1997;37:2597–2607.
56. Clark RA, Demer JL. Changes in extraocular muscle volume during ocular duction. *Invest Ophthalmol Vis Sci*. 2016;57:1106–1111.
57. Oystreck DT, Engle EC, Bosley TM. Recent progress in understanding congenital cranial dysinnervation disorders. *J Neuroophthalmol*. 2011;31:69–77.
58. Demer JL, Clark RA, Lim KH, Engle EC. Magnetic resonance imaging evidence for widespread orbital dysinnervation in dominant Duane's retraction syndrome linked to the DURS2 locus. *Invest Ophthalmol Vis Sci*. 2007;48:194–202.
59. Lennerstrand G, Schiavi C, Tian S, et al. Isometric force measured in human horizontal eye muscles attached to or detached from the globe. *Graefes Arch Clin Exp Ophthalmol*. 2006;244:539–544.
60. Snook SH, Vaillancourt DR, Ciriello VM, Webster BS. Psychophysical studies of repetitive wrist flexion and extension. *Ergonomics*. 1995;38:1488–1507.
61. David T, Smye S, James T, Dabbs T. Time-dependent stress and displacement of the eye wall tissue of the human eye. *Med Eng Phys*. 1997;19:131–139.

Investigative Ophthalmology & Visual Science

62. Shim SH, Sung KR, Kim JM, et al. The prevalence of open-angle glaucoma by age in myopia: the Korea national health and nutrition examination survey. *Curr Eye Res*. 2017;42:65–71.
63. Doucette LP, Rasnitsyn A, Seifi M, Walter MA. The interactions of genes, age, and environment in glaucoma pathogenesis. *Surv Ophthalmol*. 2015;60:310–326.
64. Leung CK, Ye C, Weinreb RN, et al. Impact of age-related change of retinal nerve fiber layer and macular thicknesses on evaluation of glaucoma progression. *Ophthalmology*. 2013; 120:2485–2492.
65. Caprioli J, Zeyen T. A critical discussion of the rates of progression and causes of optic nerve damage in glaucoma. *J Glaucoma*. 2009;18:S1–S21.
66. Rockwood EJ, Anderson DR. Acquired peripapillary changes and progression in glaucoma. *Graefes Arch Clin Exp Ophthalmol*. 1988;226:510–515.
67. Uchida H, Ugurlu S, Caprioli J. Increasing peripapillary atrophy is associated with progressive glaucoma. *Ophthalmology*. 1998;105:1541–1545.
68. Jonas JB. Clinical implications of peripapillary atrophy in glaucoma. *Curr Opin Ophthalmol*. 2005;16:84–88.
69. Witmer MT, Margo CE, Drucker M. Tilted optic disks. *Surv Ophthalmol*. 2010;55:403–428.
70. Park HJ, Hampp C, Demer JL. Longitudinal study of optic cup progression in children. *J Pediatr Ophthalmol Strabismus*. 2011;48:151–156.
71. Samarawickrama C, Mitchell P, Tong L, et al. Myopia-related optic disc and retinal changes in adolescent children from Singapore. *Ophthalmology*. 2011;118:2050–2057.
72. Vongphanit J, Mitchell P, Wang JJ. Population prevalence of tilted optic disks and the relationship of this sign to refractive error. *Am J Ophthalmol*. 2002;133:679–685.
73. Kim TW, Kim M, Weinreb RN, et al. Optic disc change with incipient myopia of childhood. *Ophthalmology*. 2012;119: 21–26.e3.
74. Jonas JB, Weber P, Nagaoka N, Ohno-Matsui K. Glaucoma in high myopia and parapapillary delta zone. *PLoS One*. 2017;12: e0175120.
75. Gupta P, Cheung CY, Saw SM, et al. Peripapillary choroidal thickness in young asians with high myopia. *Invest Ophthalmol Vis Sci*. 2015;56:1475–1481.
76. Savatovsky E, Mwanza JC, Budenz DL, et al. Longitudinal changes in peripapillary atrophy in the ocular hypertension treatment study: a case-control assessment. *Ophthalmology*. 2015;122:79–86.
77. Uhm KB, Lee DY, Kim JT, Hong C. Peripapillary atrophy in normal and primary open-angle glaucoma. *Korean J Ophthalmol*. 1998;12:37–50.
78. Budde WM, Jonas JB. Enlargement of parapapillary atrophy in follow-up of chronic open-angle glaucoma. *Am J Ophthalmol*. 2004;137:646–654.
79. Jonas JB, Naumann GO. Parapapillary chorioretinal atrophy in normal and glaucoma eyes. II. Correlations. *Invest Ophthalmol Vis Sci*. 1989;30:919–926.
80. Lee JE, Lee JY, Kook MS. Retinal nerve fiber layer damage in young myopic eyes with optic disc torsion and glaucomatous hemifield defect. *J Glaucoma*. 2017;26:77–86.
81. Lee KS, Lee JR, Kook MS. Optic disc torsion presenting as unilateral glaucomatous-appearing visual field defect in young myopic Korean eyes. *Ophthalmology*. 2014;121:1013–1019.
82. Park HY, Lee KI, Lee K, et al. Torsion of the optic nerve head is a prominent feature of normal-tension glaucoma. *Invest Ophthalmol Vis Sci*. 2015;56:156–163.
83. Rabinowitz MP, Katz LJ, Moster MR, et al. Unilateral prostaglandin-associated periorbitopathy: a syndrome involving upper eyelid retraction distinguishable from the aging sunken eyelid. *Ophthal Plast Reconstr Surg*. 2015;31:373–378.
84. Park J, Cho HK, Moon JI. Changes to upper eyelid orbital fat from use of topical bimatoprost, travoprost, and latanoprost. *Jpn J Ophthalmol*. 2011;55:22–27.
85. Filippopoulos T, Paula JS, Torun N, et al. Periorbital changes associated with topical bimatoprost. *Ophthal Plast Reconstr Surg*. 2008;24:302–307.
86. Jayaprakasam A, Ghazi-Nouri S. Periorbital fat atrophy - an unfamiliar side effect of prostaglandin analogues. *Orbit*. 2010; 29:357–359.

Investigative Ophthalmology & Visual Science